Estimated Public Health Exposure to H_2S Emissions from a Sour Gas Well Blowout in Kaixian County, China

Duoxing Yang[1*], Gangcai Chen[2], Renjian Zhang[3]

[1] *Appraisal Center for Environment and Engineering, State Environmental Protection Administration (SEPA), Beijing, 100012, China*

[2] *Chongqing Academy of Environmental Science, Chongqing, 400020, China*

[3] *Institute of Atmosphere Physics, Chinese Academy of Science, Beijing, 100029, China*

Abstract

In this study, CALPUFF was coupled with the MM5 model to estimate H_2S pollution exposure from an accidental sour well blowout. The model takes into account of detailed meteorological patterns, wet deposition and chemical transformations. An intercomparison of the performance of CALPUFF against the observed data is discussed and an examination of scatter plots and QQ plots is provided. The statistics show that the correlation coefficient and RMSE between the modeled and observed data are 0.8805 and 2.3304, respectively. The calculated H_2S concentrations are greatest close to the source, spread further downwind (approximately 20 km), and show heterogeneity characteristics. The model results also provide estimates of H_2S effects on mortality; a significant relationship was found between short-term exposure to H_2S and mortality in the process of the accidental sour well blowout. Additional key findings: public health exposure was higher in the valley than that on the mountain; model results imply that the CALPUFF coupled with the MM5 model is applicable in any setting where H_2S concentration events occur following an uncontrolled sour gas well blowout.

Keywords: MM5; CALPUFF/CALMET; Public health exposure.

---

[*]Corresponding author. Tel: 86-10-84910034, Fax: 86-10-84910838

E-*mail address*: yangduoxing@yahoo.com

INTRODUCTION

An accidental sour gas well blowout containing hydrogen sulfide (H_2S) occurred in Kaixian County of southwest China on December 23, 2003 at 22:00 local time. About 64,000 residents were evacuated from the exposure area. Statistically speaking, 243 deaths were found along with 9000 emergency room visits and hospitalization.

This paper focuses on a study to simulate and visualize the magnitude and extent of H_2S dispersion and to estimate public health exposure. Steady-state plume models, such as ISC3 (Scire *et al*., 1981; Campbell *et al*., 1998) and ADMS (Carruthers *et al*., 1999), are inapplicable in the case of this objective. The CALPUFF (Paine *et al*., 2000; Scire *et al*., 2000a) model system was more preferable. The MM5 (Grell *et al*., 1995; Bromwich *et al*., 2001) was used to provide meteorological input fields for the CALPUFF model simulation. The simulation was performed from December 23, 22:00 local time to December 24, 16:00 local time, 2003. To appraise the effects of H_2S concentrations on local public health, demographic information used was taken from the government's census.

Kaixian County is characterised by significant topographic diversity and climate variations over short distances. Strongly stratified local meteorological circulation can result in very complex surface and boundary layer meteorology. Calm conditions, surface-based upper air inversions and mesoscale thermally driven wind flow, such as mountain-valley breezes are reasonable frequent. Mountain-valley features, especially during cold, stable winter days can result in significant potential for elevated air pollution levels (Allwine *et al*., 1985; Strimaitis *et al*., 1998; Jonathan *et al*., 2002).

MODEL CONFIGURATION AND SETUP

The initial phase of CALPUFF which we used for our primary model (Scire *et al*., 1999; Paine *et al*., 2000; Bennett *et al*., 2002; Scire *et al*., 2003) involves deriving meteorological files using CALMET (Scire *et al*., 1997; Scire *et al*., 2000b; Robe *et al*., 2002), which is a diagnostic meteorological model. Much of the structure in the wind fields is determined by CALMET using its diagnostic wind field module (Douglas *et al*., 1988). As shown in Fig. 2, the basic coordinate grid for CALPUFF/CALMET consisted of 50 grid cells along the x-axis (east-west) and 50 grid cells along the y-axis (north-south), spaced 1 km apart. The coordinate system was converted to a Lambert projection grid. The ten vertical layers incorporated into the CALMET processing had heights of 20 m, 40 m, 80 m, 160 m, 300 m, 600 m, 1000 m, 1500 m, 2200 m and 3000 m. Due to lack of available meteorological observation data, the MM5 was used in this study to develop high-resolution, three-dimensional meteorological fields (i.e., wind, temperature, pressure, etc.) through FDDA simulations (Stauffer *et al*., 1994). MM5-generated meteorological fields are used

to drive the CALMET model which can use important information contained in MM5 data to resolve terrain features, such as terrain channeling and gravity-driven slope flows (Jonathan *et al.*, 2002; Zhou *et al.*, 2003). The first-guess atmosphere data for MM5 are extracted from the NCAR/NCEP FNL archives. The NCEP Final Analysis (FNL) data archived at NCAR is for every six hours at a spatial resolution of $1^o \times 1^o$ at standard pressure levels under 100 hPa. The data include two-dimensional variables, including sea surface temperature and sea level pressure, and three-dimensional variables of temperature, geopotential height, U and V components, and relative humidity. We combined a MM5 prognostic model (Douglas *et al.*, 1988) outputs with mesoscale data assimilation systems for 18 hours (December 23, 2003, 22:00:00-December 24, 2003, 16:00:00). Fig. 1 shows the model domain configuration for MM5. The model domain has 32 vertical levels, going up to about 13 km AGL, with vertical grid spacing stretched from about 20 m near the ground to 800 m near the top of the domain. This allowed CALMET to interpolate from a higher- to a lower-resolution grid (since CALMET uses ten vertical layers). One-way nesting was used to generate ambient wind fields at multiple grid-cell resolutions (27-, 9-, 3-km) as shown in Fig. 1. For each domain, the basic coordinate grid for MM5 consisted of 103 grid cells along the x-axis (east-west) and 103 grid cells along the y-axis (north-south), with the center point of the model domain set to (31.378^oN, 108.238^oE). The CALPOST (Scire *et al.*, 1999) program was used to develop concentration files. The final output of the CALPOST consisted of every 15 minutes H_2S exposure.
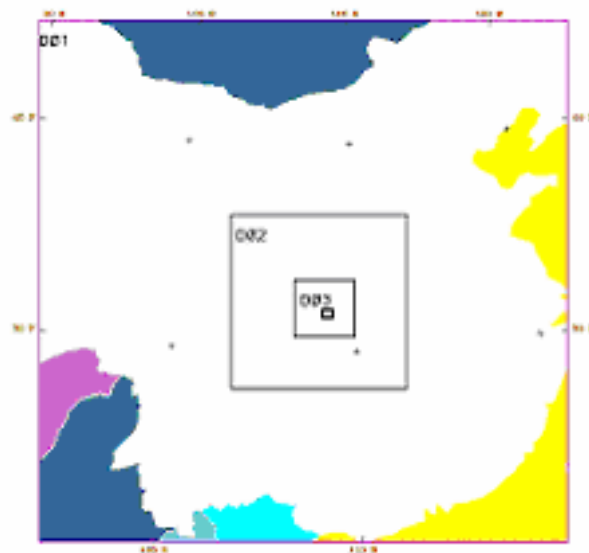
Fig. 1. MM5 Nested Computational Domain (D01: 27-km grid-cell resolution, D02: 9-km grid-cell resolution, D03: 3-km grid-cell resolution). The open box represents the location of Kaixian.

Source description

For this case study, we evaluated the impacts of the sour gas well blowout in Kaixian County on a grid approximately 50 km × 50 km (Fig. 2). We developed an emission scenario meant to reflect current emission. The content of H_2S, the averaged flux of the gas well and the stratum pressure are $150 g/m^3$, $350 \times 10^4\, m^3/d$, and 40 MPa, respectively. The emission was assumed to be uniform across the year, a simplifying assumption due to data limitations (CPI, 2005). The sour gas well, as the single isolated point source, that emits H_2S was used for this analysis. According to the method (CPI, 2005), the H_2S emission rate was determined by multiplying the content of H_2S with the well flux. The source characteristics are summarized in Table 1.
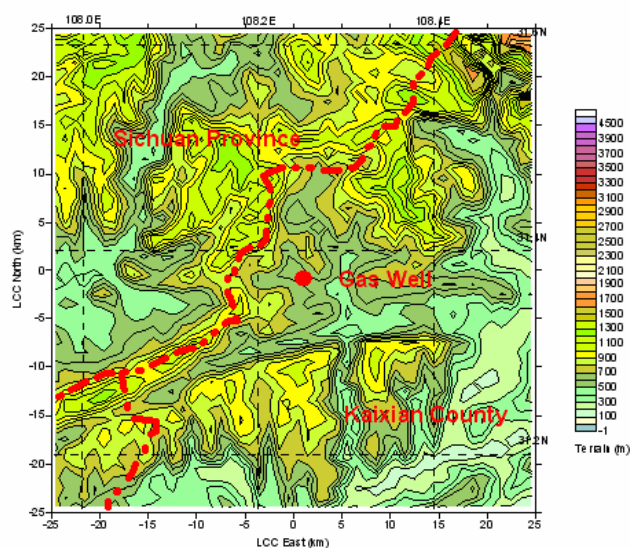
Fig. 2. CALPUFF/CALMET Domain Configuration and Terrain Elevation (county boundaries are shown by the red lines. The point source is shown by the red point).

Table 1. Point source characteristics.

Latitude (degree)	Longitude (degree)	Stack height (m)	Exit velocity (m/s)	Emission rate (g/s)
31.378	108.238	1	40	6076.39

RESULTS AND DISCUSSION

The every 15 minutes H_2S exposure during the episode was modeled for each of the 2500 grid cells. This paper discusses the model simulation results based on H_2S pollutant concentrations. We focused exclusively on model evaluation, comparisons and health exposure associated with

current emissions. Estimating health effect after the emission scenario is beyond the scope of this paper.

Model validation

The modeling system was evaluated comprehensively to ensure reasonable estimates of ambient H_2S. We present a time series of the H_2S concentrations at the monitor, which was located 1 km south of the source.. For example, Fig. 3 compares every-15-minutes values (mg/m^3) (December 24, 06:00-15:00) for the monitor against the modeled estimates for the grid cell in which that monitor is located. At first glance, the H_2S prediction seemed to be in relatively good agreement with the observed data. We further examined the statistics data, including correlation coefficient and root mean squared error (RMSE). Fig. 4 shows the scatter plots of the modeled concentrations versus the observed values. The straight line in Fig. 4 is computed by linear regression of the modeled concentrations according to the relation:

$$C_{MOD} = 1.2581C_{OBS} - 5.0545 \tag{1}$$

where C_{MOD} and C_{OBS} are the modeled and observed concentrations, respectively, in mg/m^3. Fig. 5 shows the quantile-quantile (QQ) plots of the predicted versus observed concentrations. Table 2 summarizes the statistical values for comparison. It shows that the model performed well in predicting H_2S. Note that the monitor and model are in fact providing H_2S levels at different locations, as the monitor reflects concentrations at a single point location and the modeled estimate reflects the average over a 1 km by 1 km grid cell. It also shows the difference between the modeled and the observed data. This was probably due to the fact that the emission rate varied from time to time and was not sufficiently accounted for in the emission scenario. Efforts to improve the emission invertory should be undertaken in future studies of this sort. Another plausible cause for the difference is that the wet deposition as well as chemical formation of H_2S might not be sufficiently represented in the model. Uncertainties could arise through influence of the model grid resolution on the calculated results. It should be worthwhile to examine the effect of model grid resolution on the CALPUFF predictions. Nevertheless, it is beyond the scope of this paper.
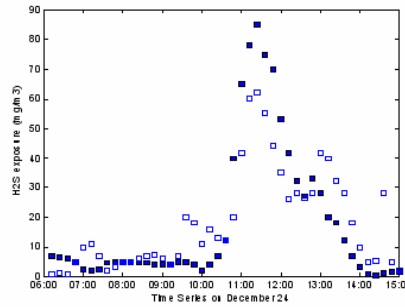
Fig. 3. Time series of CALPUFF predicted (solid box) and observed H₂S concentrations (open box) at the monitor from 06:00 to 15:00 local time, December 24, 2003 (mg/m³).
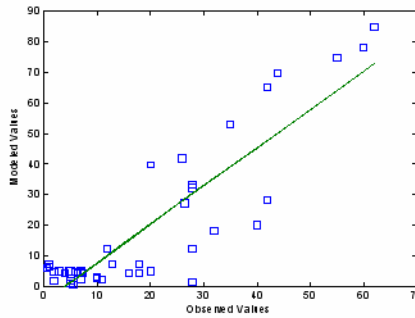
Fig. 4. Scatter plots of modeled versus observed concentrations (mg/m³).
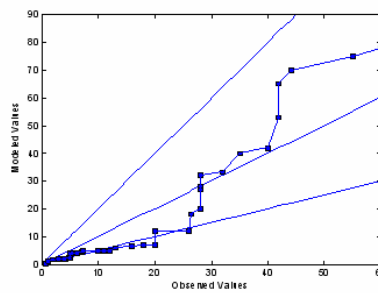
Fig. 5. Quantile-quantile plots of modeled versus observed concentrations (mg/m³).

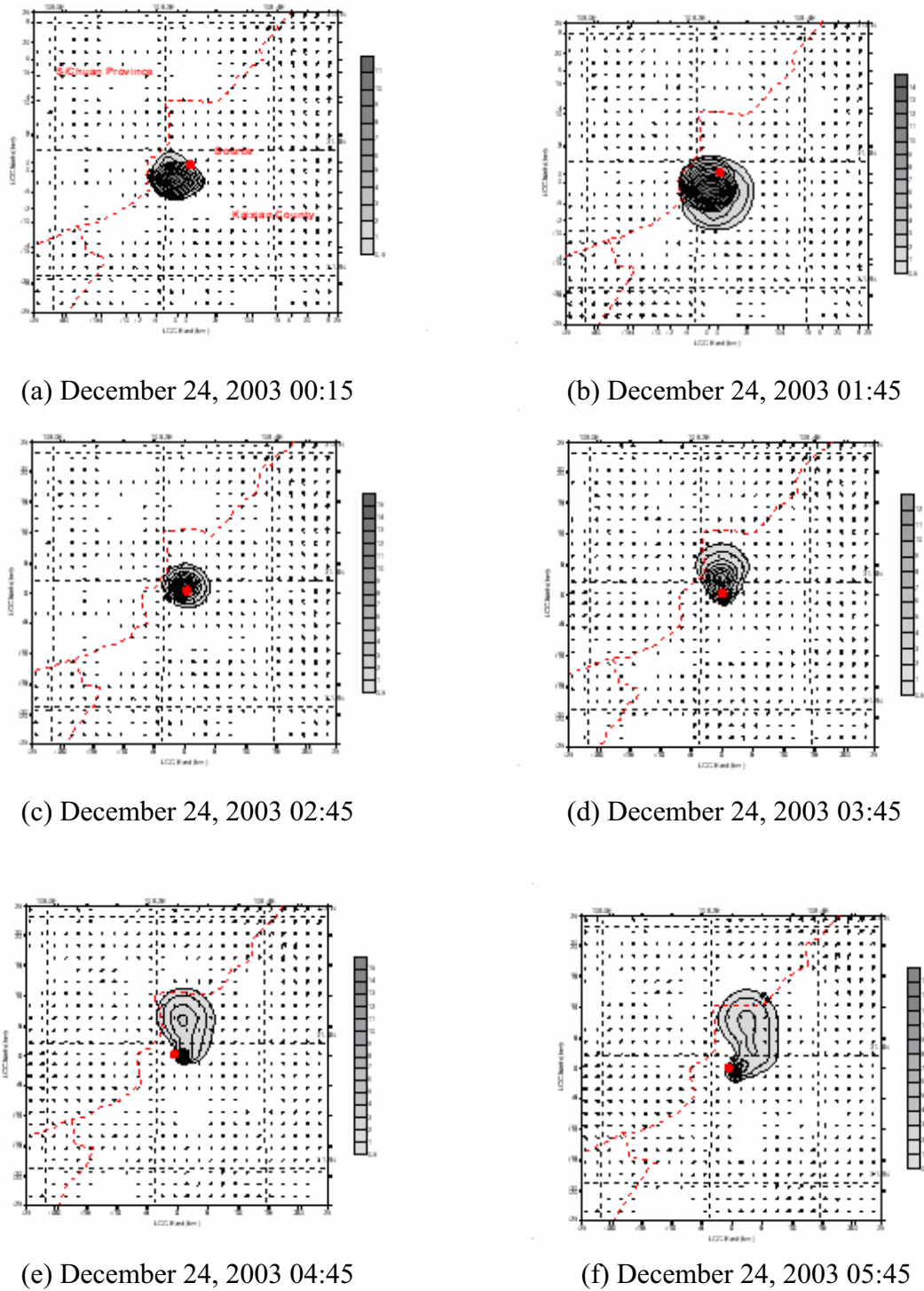**Table 2.** Statistical data of model predicted concentrations against the observed data.

Normalized correlation	Fraction of factor 2 (%)	Root mean squared error
0.8805	75.6	2.3404

H_2S concentrations and exposure

The CALPUFF simulation was performed from 10:00 local time December 23 to 16:00 December 24 over the domain described in Fig. 2. A snapshot of the horizontal distribution of winds and concentrations is presented in Fig. 6. It shows that before December 24, 11:45 local time, the CALPUFF simulation predicts concentrations mostly in the west region of Kaixian County in amounts between 0.5 and 1100 mg/m^3. The H_2S exposure mainly affected areas adjacent to the sour gas well. From 00:15 to 11:45 December 24 influenced areas gradually expand. There are some hot spots in the figures for the times 04:45, 05:45 and 07:45 north of the source. As shown in Fig. 6, the wind fields exhibit convergence in those hot spots. A strongly stratified mesoscale meteorological circulation and *in situ* convection under cold winter conditions resulted in very complex surface and boundary layer meteorology. The local circulation may be a contributing factor to those hot spots. On December 24, 11:45 local time, H_2S exposure reached to about 900 mg/m^3 and approximately 200 deaths occurred within about 1.0 km around the sour gas well.

About 14 hours after the well blowout, H_2S exposure went through the boundary and extended southwest to Sichuan Province. On December 24, 15:45 local time, H_2S exposure in southwest Sichuan ranged from 0.5 to 60 mg/m^3. H_2S concentration distributions show spatial and temporary heterogeneity due to significant topographic diversity and wind fields variations over short distances. Mountain-valley features, especially during these cold, stable winter days contributed significant potential to elevated air pollution levels. Calm conditions, surface-based upper air inversions and mesoscale, thermally driven wind flow, such as mountain-valley breezes are reasonable factors. Fig. 7 is the distribution of highest every 15-minutes H_2S exposure during the episode. It depicts the patterns and magnitudes of H_2S concentrations. The highest concentrations of H_2S occur around the gas well within 1.5 km due to the sufficient source contribution. The model predicted relatively high H_2S concentrations along the valley due to the influence of slope flow. H_2S extended over areas in southwestern Sichuan Province in concentration ranging between 0.5 and 60 mg/m^3. This shows that as the distance from the source increases, the concentrations of H_2S decrease. By comparing population distribution with H_2S concentration, we identified that approximately 60% of H_2S total exposure was located within 5 km of the sour gas well, around which maximal impacts are centered. It's clear that H_2S exposure mainly dispersed along the valley, which contributed mainly to mortality and hospitalization resulting from the accident. Given the complex terrain and wind fields variation affecting air pollution distribution (Douglas *et al.*, 1988, Perry *et al.*, 1989), the concentration distributions show the heterogeneity patterns in spatial and temporal scales. The mortality due to the blowout were higher in the valley than the mountain; because H_2S is heavier than air, it tends to accumulate in low-lying areas. Citizens inhaling air containing toxic hydrogen sulfide vapor were

fatally injured because the combination of hydrogen sulfide concentration and time of exposure exceeded the lethal threshold (Jonathan *et al.*, 2002). The lethal threshold for H_2S is 900 mg/m^3. People were fatally poisoned after 30 minutes of exposure.
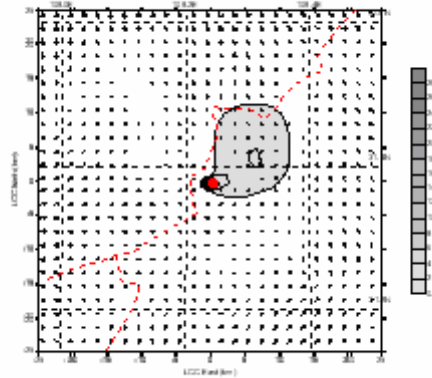

(a) December 24, 2003 00:15

(b) December 24, 2003 01:45

(c) December 24, 2003 02:45

(d) December 24, 2003 03:45

(e) December 24, 2003 04:45

(f) December 24, 2003 05:45

Fig. 6. (a-f) Spatial and temporal distribution of predicted H_2S concentrations at each receptor (mg/m^3).
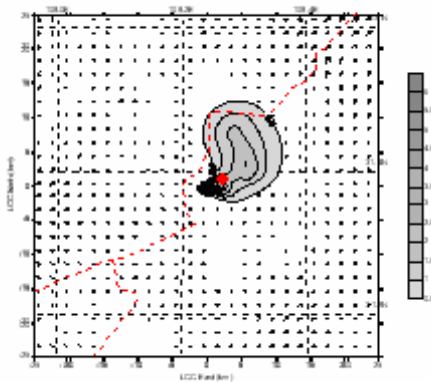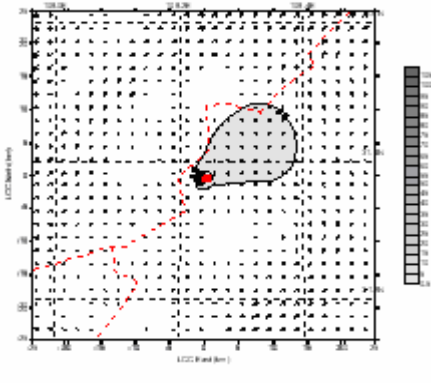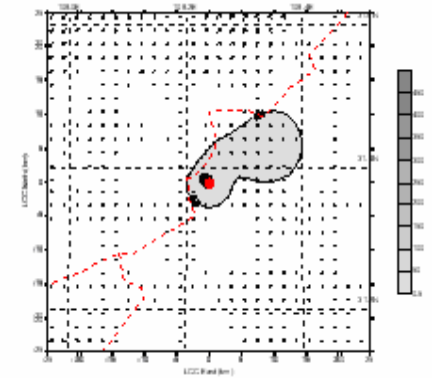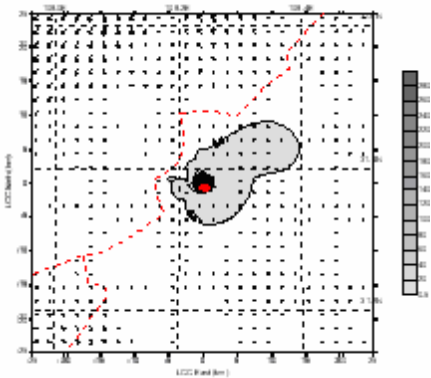
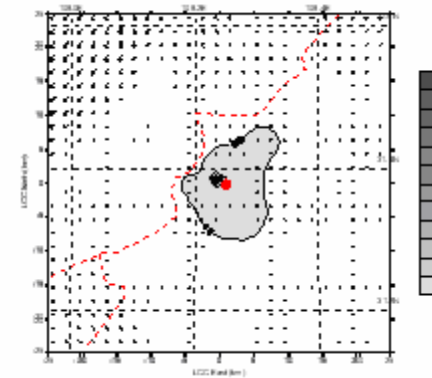(g) December 24, 2003 06:45

(h) December 24, 2003 07:45

(i) December 24, 2003 08:45
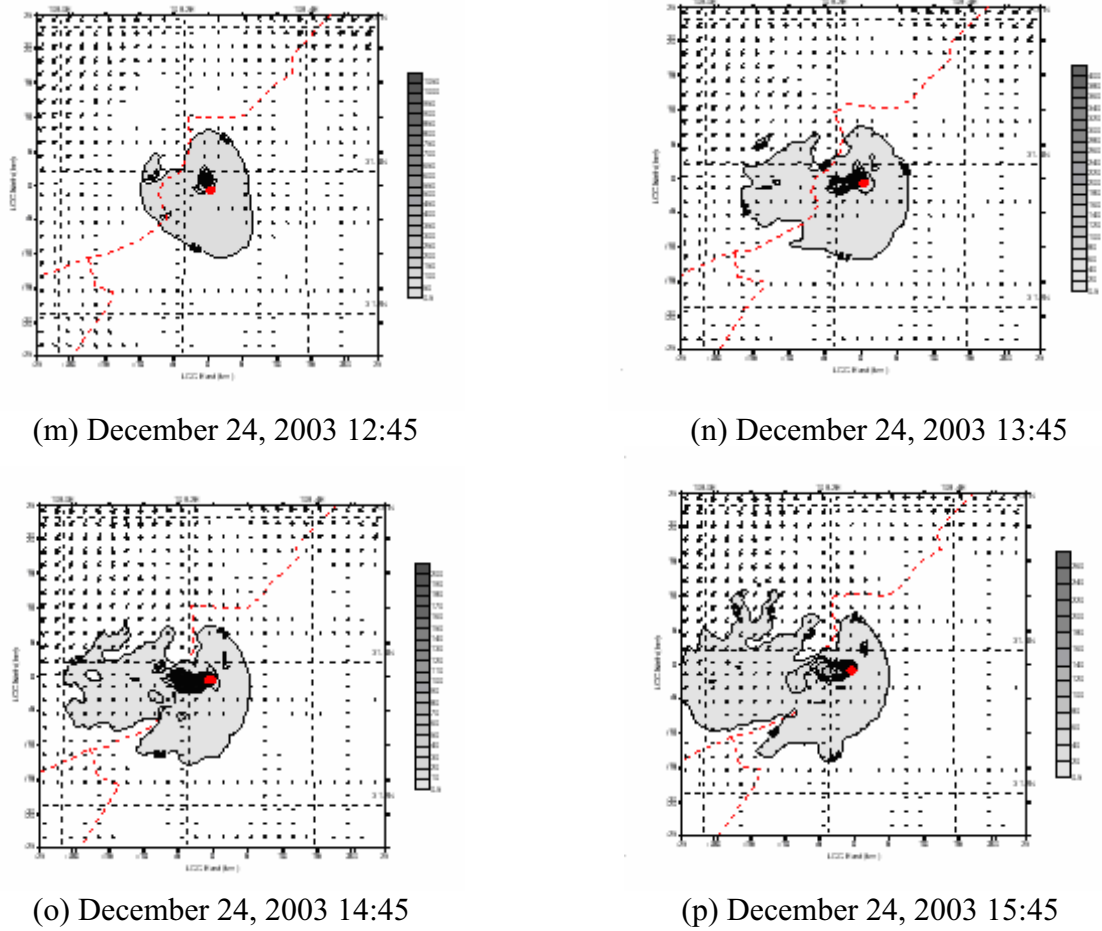
(j) December 24, 2003 09:45

(k) December 24, 2003 10:45

(l) December 24, 2003 11:45

Fig. 6. (g-l) Spatial and temporal distribution of predicted H_2S concentrations at each receptor (mg/m^3).

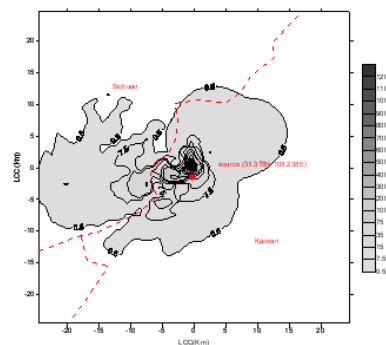| (m) December 24, 2003 12:45 | (n) December 24, 2003 13:45 |
| (o) December 24, 2003 14:45 | (p) December 24, 2003 15:45 |

Fig. 6. (m-p) Spatial and temporal distribution of predicted H_2S concentrations at each receptor (mg/m^3).

Fig. 7. Predicted highest 15-minute average H_2S concentrations at each receptor during the sour gas well blowout (mg/m^3).

Table 3. Hydrogen sulfide (H_2S) established dose-effect relationships.

Effect	H_2S Concentration (mg/m^3)
Immediate collapse with paralysis of respiration	1400-2800
Strong CNS stimulation, hyperpnoea , respiratory arrest	750-1400
Pulmonary edema with risk of death	450-750
Loss of olfactory sense	210-350
Serious eye damage	70-140
Threshold for eye irritation	15-30

To translate H_2S concentrations from the sour well release into estimated adverse health effects, demographic information taken from the local government census is combined with epidemiological studies (World Health Organization, 1981) that have estimated concentration-response relationships. Population density is 32 persons/km^2 within 5 km surrounding the sour gas well. At concentrations of 15 mg/m^3 and above, hydrogen sulfide causes conjunctival irritation. Serious eye damage is caused by a concentration of 70 mg/m^3. At higher concentrations (above 225 mg/m^3), hydrogen sulfide has a paralyzing effect on the olfactory perception. At higher concentrations, respiratory irritation is the predominant symptom, and at a concentration of around 400 mg/m^3 there is a risk of pulmonary edema. At even higher concentrations there is strong stimulation of the central nervous system, with hyperpnoea leading to apnea, convulsions, unconsciousness, and death. At concentrations of over 1400 mg/m^3 there is immediate collapse. In fatal intoxication cases, brain edema, degeneration and necrosis of the cerebral cortex and the basal ganglia have been observed.

Dose-effect and dose-response relationship was examined. The first noticeable effect of hydrogen sulfide at low concentrations is its unpleasant odor. Conjunctival irritation is the next subjective symptom and can cause so-called "gas eye" at hydrogen sulfide concentrations of 70-140 mg/m^3. Table 3 shows the established dose-effect relationships for hydrogen sulfide. People exposed to hydrogen sulfide concentrations of less than 30 mg/m^3 are reported to have rather diffuse neurological and mental symptoms. On the other hand, changes of haem synthesis have been reported at concentrations of less than 7.8 mg/m^3. It is not known whether the inhibition is caused by low concentration levels or by the cumulative effects of occasional peak concentrations. It can be seen from Figures 6 and 7 that H_2S exposure dominated in the valleys extending southwest and southeast, as well as north, which was consistent with reported mortality and hospitalization. Of the total number of people affected 2.73% occurred within 2 km of the sour gas well, since more than 90% of affected individuals live beyond 2 km of the sour well. However, 90% of the deaths happened within 1.5 km of the sour gas well, due primarily to higher H_2S exposure. Note that the exposure estimates generated here are for individual exposure

based only on a specific fixed location, which didn't incorporate movement from work to home, indoors and outdoors and so on. What's more, the exposure estimates generated here are strongly restricted to the period of the gas well blowout.

CONCLUSIONS

A CALPUFF coupled with MM5 model is presented and used to study H_2S exposure from a sour gas well blowout. The model performed quite well in predicting the H_2S exposure compared against observations. The calculated H_2S estimates display significant spatial and temporal heterogeneity. The highest H_2S exposure was located within 1.5 km diameter around the sour gas well, with concentration ranging from 60 to 1200 mg/m^3. The sour gas well blowout also contributed highly to H_2S exposure in southwest Sichuan Province in amounts between 0.5 and 60 mg/m^3. The H_2S exposure dominated in the valleys extending southwest and southeast, as well as north, consistent with mortality and hospitalization related to the accident. Statistics show that of the total number of affected 2.73% occurred were within 2 km from the source, while 90% of the deaths happened within 1.0 km, due to high H_2S exposure. This study illustrates that in such complex terrain lacking available observed meteorological data, the CALPUFF coupled with MM5 model can provide meaningful information for emergency management purposes.

ACKNOWLEDGMENTS

REFERENCES

Allwine, K.J., and Whiteman, C.D. (1985). MELSAR: *A Mesoscale Air Quality Model for Complex Terrain: Vol. 1--Overview, Technical Description and User's Guide.* Pacific Northwest Lab, Richland, WA.

Bennett, M.J., M.E., Yansura, I.G., Hornyik, J.M., Nall, D.G., and Ashmore, C.G. (2002). Evaluation of the CALPUFF Long-range Transport Screening Technique by Comparison to Refined CALPUFF Results for Several Power Plants in Both the Eastern and Western United States. Proceedings of the Air & Waste Management Association's 95th Annual Conference, June 23-27, 2002; Baltimore, MD. Paper #43454.

Bromwich, D.H., Cassano, T. Kelin, G. Heinemann, K.M., Hines, K. Steffen and Box, J.E. (2001). Mesoscale Modeling of Katabatic Winds over Greenland with the Polar MM5. *Mon.*

Wea. Rev. 129: 2290-2309.

Campbell, S.A. (1998). Gas Scavenging Coefficients for Use in the ISC3 Wet Deposition\Algorithms. Paper 98-TAB.05P. Air & Waste Management Association 91th Annual Meeting & Exhibition, San Diego, California, USA. 14-18 June 1998.

Carruthers, D.J., McKeown, A.M., Hall, D.J., and Porter S. (1999). Validation of ADMS Against Wind Tunnel Data of Dispersion from Chemical Warehouse Fires. *Atmos. Environ.* 33: 1937-1953.

CPI (China Petrol Institute of South-West Oil and Gas Exploring Corporation). (2005). Environmental impact assessment report.

Douglas, S. and Kessler, R. (1988). User's Guide to the Diagnostic Wind Model, California Air Resources Board, Sacramento, CA.

Grell, G.A., Dudhia, J., and Stauffer, D.R. (1995). *A Description of the Fifth Generation Penn State/NCAR Mesoscale Model (MM5)*. NCAR Tech. Note, CAR/TN-398+STR, 122 pp. References 9-2.

Jonathan, I.L., Spenglera, D., and Hlinkab, D. (2002). Using CALPUFF to Evaluate the Impacts of Power Plant Emissions in Illinois: Model Sensitivity and Implications. *Atmos. Environ.* 36: 1063–1075.

Paine, R.J., and Heinold, D.W. (2000). Issues Involving Use of CALPUFF for Long-range Transport Modeling. Presented at the Air and Waste Management Association 93rd Annual Meeting and Exhibition, Salt Lake City, UT, June 2000.

Perry, S.G., Burns, D.J., Adams, L.H., Paine, R.J., Dennis, M.G., Mills, M.T., Strimaitis, D.G., Yamartino, R.T, and Insley, E.M. (1989). User's Guide to the Complex Terrain Dispersion Model Plus Algorithms for Unstable Situations (CTDMPLUS) Volume 1: Model Description and User Instructions. EPA/600/8-89/041, U.S. Environmental Protection Agency, RTP, NC.

Robe, F.R., Wu, Z.X., and Scire, J.S. (2002). Real-time SO_2 Forecasting System with Combined ETA Analysis and CALPUFF Modeling. Proceedings of the 8th International Conference on Harmonisation within Atmospheric Dispersion Modelling for Regulatory Purposes, 14-17 October 2002, Sofia, Bulgaria.

Scire, J.S., Strimaitis, D.G., Yamartino, R.J. (1999). A User's Guide for the CALPUFF Dispersion Model (Version 5.0). *Earth Tech*, Concord, MA.

Scire, J.S., and Schulman, L.L.. (1981). Evaluation of the BLP and ISC Models with SF6 Tracer Data and SO_2 Measurements at Aluminum Reduction Plants. Specialty Conference on Dispersion Modeling from Complex Sources, April 7-9, St. Louis, MO.

Scire, J.S., and Robe, F.R. (1997). Fine-Scale Application of the CALMET Meteorological Model to a Complex Terrain Site. Paper 97-A1313. Air & Waste Management Association 90th Annual Meeting & Exhibition, Toronto, Ontario, Canada. 8-13 June 1997.

Scire, J.S., Robe, F.R., Fernau, M.F., and Yamartino, R.J. (2000a). A User's Guide for the

CALMET Meteorological Model (Version 5). *Earth Tech, Inc.,* Concord, MA.

Scire, J.S., Strimaitis, D.G., and Yamartino, R.J. (2000b). A User's Guide for the CALPUFF Dispersion Model (Version 5). *Earth Tech, Inc.,* Concord, MA.

Scire, J.S., Wu, X.Z., and Moore, G.E. (2003). Evaluation of the CALPUFF Model in Predicting Concentration, Visibility and Deposition Impacts at Class I Areas in Wyoming. A&WMA Specialty Conference, Guideline on Air Quality Models: The Path Forward, 22-24 October 2003, Mystic, CT.

Strimaitis, D.G., Scire, J.S., and Chang, J.C. (1998). Evaluation of the CALPUFF Dispersion Model with Two Power Plant Data Sets. Preprints 10th Joint AMS/AWMA Conference on the Applications of Air Pollution Meteorology, 11-16 January 1998, Phoenix, Arizona.

Stauffer D.R., and Seaman, N.L. (1994). Multiscale Four Dimensional Data Assimilation, *J. Appl. Met.* 33: 416-434.

World Health Organization. (1981). Hydrogen Sulfide (Environmental Health Criteria, No. 19). Geneva.

Zhou, Y, Levy, J.I., Hammitt, J.K., and Evans, J.S. (2003). Estimating Population Exposure to Power Plant Emissions Using CALPUFF: A Case Study in Beijing, China. *Atmos. Environ.* 37: 815-826.